

Generating multi-layer nested chaotic attractor and its FPGA implementation

Xuenan Peng(彭雪楠), Yicheng Zeng(曾以成), Mengjiao Wang(王梦蛟), and Zhijun Li(李志军)
Citation: Chin. Phys. B, 2021, 30 (**6**): 060509. DOI: 10.1088/1674-1056/abda34
Journal homepage: http://cpb.iphy.ac.cn; http://iopscience.iop.org/cpb

What follows is a list of articles you may be interested in

Fractal sorting vector-based least significant bit chaotic permutation for image encryption

Yong-Jin Xian(咸永锦), Xing-Yuan Wang(王兴元), Ying-Qian Zhang(张盈谦), Xiao-Yu Wang(王晓雨), and Xiao-Hui Du(杜晓慧)
Chin. Phys. B, 2021, 30 (**6**): 060508. DOI: 10.1088/1674-1056/abda35

An image encryption algorithm based on improved baker transformation and chaotic S-box

Xing-Yuan Wang(王兴元) , Huai-Huai Sun(孙怀怀) , and Hao Gao(高浩)
Chin. Phys. B, 2021, 30 (**6**): 060507. DOI: 10.1088/1674-1056/abdea3

Control of chaos in Frenkel-Kontorova model using reinforcement learning

You-Ming Lei(雷佑铭) and Yan-Yan Han(韩彦彦)
Chin. Phys. B, 2021, 30 (**5**): 050503. DOI: 10.1088/1674-1056/abd74f

A multi-directional controllable multi-scroll conservative chaos generator: Modelling, analysis, and FPGA implementation

En-Zeng Dong(董恩增), Rong-Hao Li(李荣昊), and Sheng-Zhi Du(杜升之)
Chin. Phys. B, 2021, 30 (**2**): 020505. DOI: 10.1088/1674-1056/abc239

A novel method of constructing high-dimensional digital chaotic systems on finite-state automata

Jun Zheng(郑俊), Han-Ping Hu(胡汉平)
Chin. Phys. B, 2020, 29 (**9**): 090502. DOI: 10.1088/1674-1056/aba60f

---

Generating multi-layer nested chaotic attractor and its FPGA implementation*

Xuenan Peng(彭雪楠)[1], Yicheng Zeng(曾以成)[1,†], Mengjiao Wang(王梦蛟)[2], and Zhijun Li(李志军)[2]

[1] School of Physics and Optoelectronic Engineering, Xiangtan University, Xiangtan 411105, China
[2] School of Automation and Electronic Information, Xiangtan University, Xiangtan 411105, China

(Received 2 December 2020; revised manuscript received 9 January 2021; accepted manuscript online 11 January 2021)

Complex chaotic sequences are widely employed in real world, so obtaining more complex sequences have received highly interest. For enhancing the complexity of chaotic sequences, a common approach is increasing the scroll-number of attractors. In this paper, a novel method to control system for generating multi-layer nested chaotic attractors is proposed. At first, a piecewise (PW) function, namely quadratic staircase function, is designed. Unlike pulse signals, each level-logic of this function is square constant, and it is easy to realize. Then, by introducing the PW functions to a modified Chua's system with cubic nonlinear terms, the system can generate multi-layer nested Chua's attractors. The dynamical properties of the system are numerically investigated. Finally, the hardware implementation of the chaotic system is used FPGA chip. Experimental results show that theoretical analysis and numerical simulation are right. This chaotic oscillator consuming low power and utilization less resources is suitable for real applications.

Keywords: multi-layer nested attractors, composited attractors, multi-scroll attractors, FPGA realization

PACS: 05.45.Gg, 05.45.Pq, 05.45.–a **DOI:** 10.1088/1674-1056/abda34

1. Introduction

Chaos phenomenon is widespread existences in nature. On the one hand, chaos phenomenon is undesirable in some fields like construction engineering, because any tiny disturbance may result in fatal disaster. On the other hand, researchers need more complex chaotic consequences to achieve practical applications, such as chaos-based encryption schemes.[1,2] The multi-scroll chaotic attractor is considered as a manifestation of the system having complex dynamic behaviors. Obtaining multi-scroll chaotic systems can be summarized as the following two parts.

One is to design novel chaotic systems and modifying an existing chaotic system.[3–5] A four-dimensional (4D) smooth quadratic autonomous system, constructed by a linear controller to a three-dimensional (3D) pseudo four-wing system, was proposed.[6] A 4D cyclic symmetry chaotic system with multi-stability and coexisting attractors was designed.[7] The 4D systems have vast key spaces, but need more resources to implement them. Thus, lower dimensional chaotic systems with complex behaviors have been widely researching in recent years.[8,9] A 3D chaotic system with trigonometric function as a nonlinear controller for generating hidden and self-excited attractor was proposed.[10] Fractional-order chaotic systems are extremely useful to describe many real-world phenomena.[11] A 3D fractional-order chaotic system generating one to four wing controllable chaotic attractor was reported.[12] A fractional order dynamical system with a variable double-scroll attractor on a line, lattice, and 3D grid was introduced.[13] However, it is difficult to reconstruct a novel chaotic system with more complex dynamical behaviors. Moreover, these systems only generate chaotic attractors with a limited number of scrolls.

Another method is introducing nonlinear functions into chaotic models to obtain multi-scroll attractors.[14–17] The hyperbolic tangent function series was designed for generating multi-scroll attractor.[18] By using offset boosting technique and introducing absolute-value function, the number of coexisting attractors in the chaotic system can be doubled.[19] A Chua's diode with multi-segment piecewise linearity was designed for generating multi-scroll Chua's attractors.[20] Recently, a technique based on non-autonomous functions for generating multi-scroll attractors was proposed.[21] Multi-double-scroll attractors were generated by adding multi-level-logic pulse excitation in double-wing chaotic systems.[22] By using non-autonomous approaches, the modified Sprott C system creating multi-scroll hidden attractors was reported.[23] Sigmoid function was used to control system generating multi-scroll hidden chaotic attractor.[24] Obtaining various types multi-scroll attractors was extensively researched, but the methods for increasing the number of nested chaotic attractors have not been reported.

In this paper, we introduce a non-autonomous approach to create multi-layer nested attractor in modified Chua's system. The PW function plays a critical role in non-autonomous approaches. Most works only use one PW function to control chaotic system. But, due to modified Chua's system having

*Project supported by the National Natural Science Foundation of China (Grant No. 62071411).
†Corresponding author. E-mail: yichengz@xtu.edu.cn
© 2021 Chinese Physical Society and IOP Publishing Ltd

second power and third power nonlinear terms, we need to design 'staircase function' and 'quadratic staircase function' to control the system. Then, the steps for creating multi-layer nested attractor are elaborated. Great majority nested attractor merely has one layer, while our method can create three-layer even multi-layer nested attractor. Meanwhile, the novel chaotic oscillator is coded in FPGA chip by employing Verilog HDL. As compared with original system, we can obtain more complex chaotic sequences with little increased consumption of resources. The rest part of this paper are organized as follows: in Section 2, the quadratic staircase function is designed. A chaotic model is proposed and analyzed in Section 3. The FPGA realization of these chaotic models is displayed in Section 4. Finally, some conclusions are included in the last section.

2. Quadratic staircase function

The pulse signal $f_i(t)$ is expressed as follows:

$$f_i(t) = \begin{cases} 1, & \phi_i + nT < t \le \phi_i + nT + \tau, \\ 0, & \phi_i + nT + \tau < t \le \phi_i + (n+1)T. \end{cases} \tag{1}$$

where, T is period, τ is pulse-width, and ϕ_i is start time. The duty ratio is defined as 0.5. And the quadratic staircase function $Q(t)$ is the summation of squares of N pulse signal $f_i(t)$ and is written as follows:

$$Q(t) = (\sum_{i=1}^{N} f_i(t) + 1)^2. \tag{2}$$

According to the above equation, the level-logic of $Q(t)$ is $(N+1)^2, N^2, (N-1)^2, \ldots, 2^2, 1$. The time series of the above functions are plotted in Fig. 1.

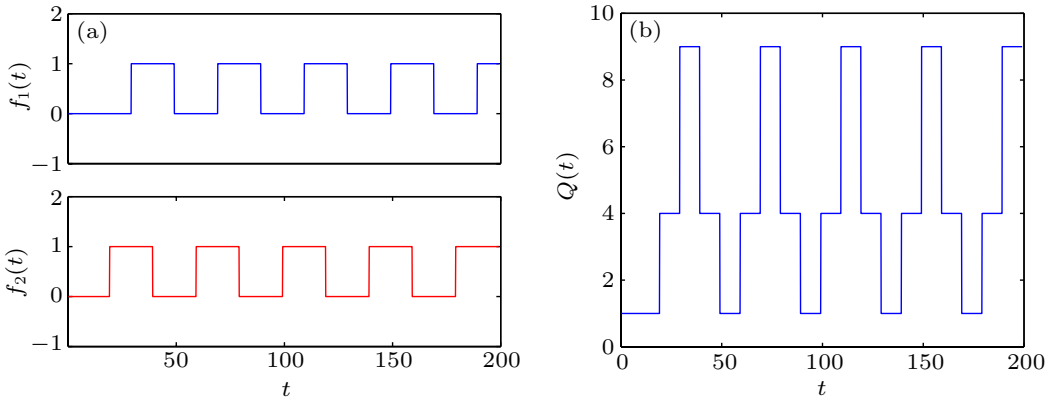


Fig. 1. Time series of nonlinear functions. (a) Pulse signal with different start time ($T = 40$, $\phi_1 = 0$, $\phi_2 = \tau/2$). (b) Quadratic staircase function got by $(f_1(t) + f_2(t))^2$.

3. Multi-layer nested chaotic attractor

3.1. Chaotic model

In this section, by introducing PW function to modified Chua's system with nested attractor, multi-layer nested chaotic system is constructed. Firstly, the modified Chua's system has eight terms including three nonlinear terms.[4] The equations are expressed as follows:

$$\begin{cases} \dot{x} = 6.8(y - 0.6x - ax^3 + bx|x|), \\ \dot{y} = x + z, \\ \dot{z} = -15.1y + c\,\mathrm{sgn}(x), \end{cases} \tag{3}$$

where x, y, and z are state variables and parameters a, b, and c are constants. The parameters are set to $a = 0.45$, $b = 1.1$ and $c = 1$ in Ref. [4]. Here, we concisely exhibit the dynamics of this system. The Lyapunov exponents' spectrums and bifurcation diagrams *versus* parameters a and b are shown in Fig. 2. Dynamics of system (3) exhibited by spectrum are almost the same as bifurcation diagram displaying. When $a > 0.5$ or $b < 1.1$, chaotic mapping area of system (3) decreases gradually.

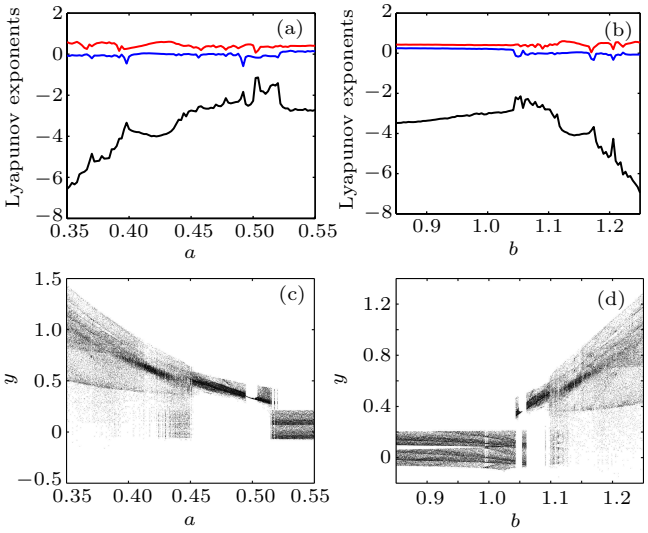


Fig. 2. (a) Lyapunov exponents' spectrum *versus* parameter a ($b = 1.1$, $c = 1$). (b) Lyapunov exponents' spectrum *versus* parameter b ($a = 1.1$, $c = 1$). (c) Bifurcation diagram varying with parameter a. (d) Bifurcation diagram varying with parameter b.

Then, considering following transformation: by substituting $-z$ into z, the correspond $\dot{z}$ will change to $-\dot{z}$. Transforming different state variables will result in system generating attractor symmetric about different planes. For ease to observe

the results, we merely choose state variable z. The transformed system (3) is written as follows:

$$\begin{cases} \dot{x} = 6.8(y - 0.6x - ax^3 + bx|x|), \\ \dot{y} = x - z, \\ \dot{z} = 15.1y - c\mathrm{sgn}(x). \end{cases} \tag{4}$$

The novel system (4) can create chaotic attractors which is mirror symmetric with original one. The mirror symmetric attractor generated by system (4) (colored in red) and original attractor created by system (3) (colored in blue) are shown in Fig. 3(a). Through this converting, a pair of symmetric attractors, which are also called two-layer attractor with one-layer nested attractor, are created. For any systems with nested attractors, changing their state variables, can create one-layer nested attractors in phase portrait.

For generating multi-layer nested attractor, we consider the following transformation: $x = eX, y = eY, z = eZ$ (e is a real constant). The system (3) will transform to

$$\begin{cases} \dot{X} = 6.8(Y - 0.6X - ae^2X^3 + beX|X|), \\ \dot{Y} = X - Z, \\ \dot{Z} = 15.1Y - c\,\mathrm{sgn}(X)/e. \end{cases} \tag{5}$$

We note that the coefficient of cubic term is e^2, while quadratic term is e and symbolic function term is $1/e$. Through adjusting the value of parameter e, the system (3) can generate different amplitude attractors as plotted in Fig. 3(b). There are four-layer chaotic attractors generated by the above system with different parameter e, which contain three-layer nested attractors. For different systems, the position and the number of parameter e may be different. In Fig. 3(c), the order of attractors from outside to inside is: four normal size outside scrolls ($e = 1$), four small size outside scrolls ($e = 2$), four normal size inner scrolls ($e = 1$), and four small size inner scrolls ($e = 2$).

In the following work, we use non-autonomous method to combine these attractors for generating multi-layer nested attractors. Introducing three different types of PW function to system (3), we can get novel equations as expressed below:

$$\begin{cases} \dot{x} = 6.8(y - 0.6x - aQ(t)x^3 + b(f(t)+1)x|x|), \\ \dot{y} = x + P(t)z, \\ \dot{z} = -P(t)15.1y + cP(t)\mathrm{sgn}(x)/(f(t)+1), \end{cases} \tag{6}$$

where, $P(t)$ is pulse function proposed by Hong *et al.*[20] It is expressed as $\mathrm{sgn}(\sin(0.005t))$. $P(t)$ is used to control system creating mirror symmetric attractors. $Q(t)$ and $f(t)$ control the amplitude of attractors generated by the system. When $a = 0.1125$, $b = 0.55$, $c = 2$, $T_Q = T_f = 600$, the multi-layer attractors generated by system (6) are shown in Fig. 3(d).

The method to generate multi-layer nested attractors can be summarized as follows: (i) chaotic system having nested attractors; (ii) through changing sign of arbitrary state variables to create mirror symmetry attractors; (iii) shrinking the amplitude of attractors by compression state variables; (iv) using pulse signal to control chaotic system for combining the above attractors.

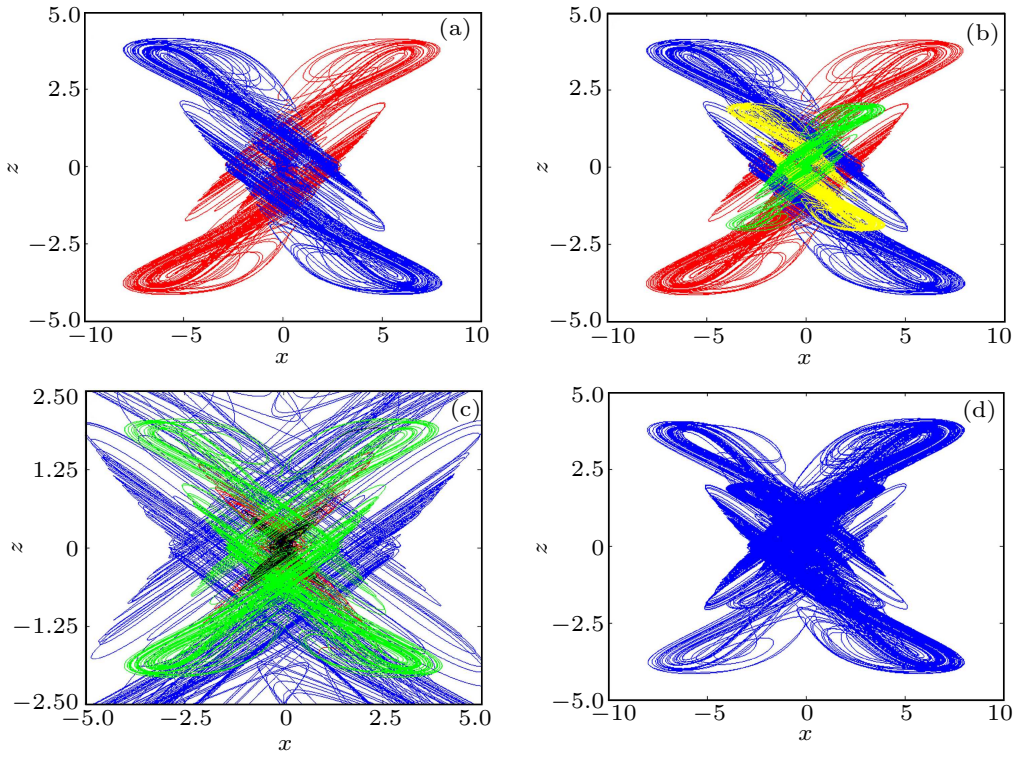


Fig. 3. (a) Mirror symmetry attractors ($a = 0.1125$, $b = 0.55$, $c = 2$). (b) Mirror symmetry attractors and different amplitude attractors (compressed original attractor colored in yellow, compressed mirror image attractor colored in green). (c) Partial enlarged view of multi-layer nested attractor (first layer colored in blue, second layer colored in green, third layer colored in red, the last layer colored in black). (d) Multi-layer nested Chua's attractor under initial condition ($x_0 = 0.1$, $y_0 = 0.3$, $z_0 = 0.2$).

3.2. Dynamics analysis of system with multi-layer nested attractor

By setting the left-hand side of the chaotic system (6) to zero, twenty-five equilibrium points exist: $S_0(0,\ 0,\ 0)$, S_{1-4} $(-0.578e,\ -0.066e,\ \pm 0.578e)$, S_{5-8} $(0.578e,\ 0.066e,\ \pm 0.578e)$, S_{9-12} $(-1.718e,\ -0.066e,\ \pm 1.718e)$, S_{13-16} $(1.718e,\ 0.066e,\ \pm 1.718e)$, $S_{17-20}(0.148e,\ 0.066e,\ \pm 0.148e)$, and S_{21-24} $(-0.148e,\ -0.066e,\ \pm 0.148e)$, where the value of parameter e is 1 or 2. The distribution of equilibrium point projection on x–z plane is shown in Fig. 4(a). The Jacobian matrix of the linearized system (6) is expressed as follows:

$$J = \begin{bmatrix} -6.8h(x) & 6.8 & 0 \\ P(t) & 0 & P(t) \\ 2\delta(x)/(f(t)+1) & -15.1P(t) & 0 \end{bmatrix}, \tag{7}$$

where $h(x)$ is written as $0.6-3aQ(t)x^2+b(f(t)+1)\beta(x)$. By solving characteristic equation of the matrix J, the eigenvalues of the equilibrium point are tabulated in Table 1. E_0 and E_{9-24} are unstable index-2 saddle-focus points having one negative real root and two complex conjugate roots with positive real part; E_{1-8} are unstable index-1 saddle points with two negative real root and a positive real root. The Lyapunov exponents' spectrum is plotted in Fig. 4(b). Obviously, the Lyapunov exponents have hardly changed. This means that our method only changes the phase space orbits of the attractor, not the chaotic state.

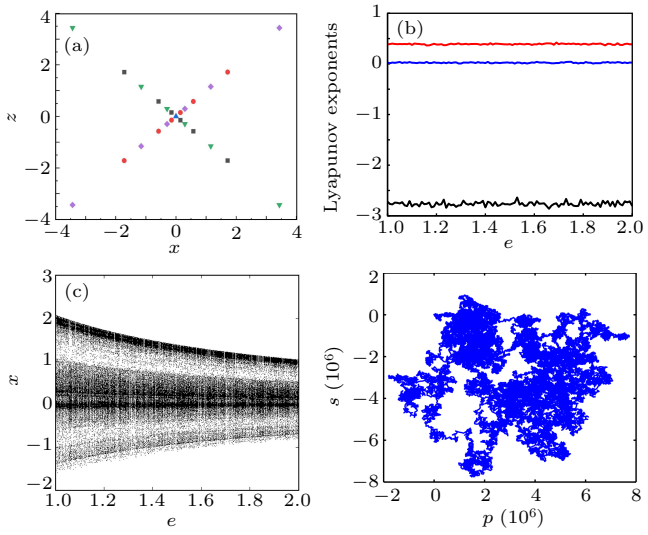


Fig. 4. Distribution of equilibrium points (original attractor colored in green, mirror symmetry attractor colored in purple, compressed original attractor colored in black, compressed mirror symmetry attractor colored in red). (b) Lyapunov exponents' spectrum varying with parameter e. (c) Bifurcation diagram varying with parameter e. (d) 0–1 test of the system.

For further analyses of the chaoticity of the system (6), the bifurcation diagram and the 0–1 test are shown in Figs. 4(c) and 4(d). Similar to the above conclusions, the bifurcation diagram exhibits the amplitude of the chaotic attractor decreasing. And the system (6) exhibits the irregular Brownian motion in the p–s plane when $(x_0, y_0, z_0) = (0.1, 0.3, 0.2)$. Thus, the system is of the chaoticity in this condition. Moreover, the axis scales of the figure are bigger than other systems, it means the system has better randomness. According to the Table 1 and Fig. 4, the sign transformation of the state variable and the proportional compression have not affected the chaoticity of the system.

Table 1. Eigenvalues of equilibrium point.

Equilibrium points	Eigenvalue 1	Eigenvalues 2,3
E_0	–4.565	0.242 ∓ 3.233i
E_{1-8}	2.261	-0.380 ∓ 3.142i
E_{9-16}	–6.258	0.392 ∓ 3.613i
E_{17-24}	–2.906	0.419 ∓ 3.250i

4. FPGA realization

Digital circuits realization of the chaotic system has been researched in recent years. Recently, various 2D sine chaotic maps were realized by using microcontroller MSP430F249.[25,26] Similarly, chaos-based secure communication system employing microcontroller was designed.[27] However, as compared with microcontroller, FPGA has more benefit such as parallel calculation, easy to use numerous IP cores, and so on. Thus, FPGA-based chaotic oscillator attracted widely interest.[28–31] In this section, we employ Runge–Kutta (RK-4) numerical method and fixed-point number (1-bit signal part, 7-bit integer part, 24-bit decimal part) to implement system (6).

4.1. Verilog HDL encoding

State machine method is a common method to realize chaotic system in Verilog HDL programming.[32] The state machine to implement modified Chua's system include eleven states: S_0–S_{10}. Where, S_0–S_6: calculate the iterate results; S_7–S_8: implementing RK-4 numerical method; S_9: adding a positive offset into results generated by S_8; S_{10}: truncating 32-bit outputs to 14-bit for adapting DAC input. Implementation of the novel chaotic system needs extra two states: S_{E1}, S_{E2}. S_{E1}: According to the logic level of PW function $P(t)$, selecting the chaotic model for iterating in system (3) or system (4) (logic '0' denoting system (3), logic '1' denoting system (4)). S_{E2}: according to the logic level of staircase functions to determine the value of parameter e. There are two values of 1-bit register: 0 and 1. Modified Chua's oscillator module can perceive these values and make different operations. For example, when register outputting value 1, the equation $4ax^3$ is calculated in the module, otherwise the expression is ax^3. Therefore, the quadratic staircase function is not directly implemented in this method. The state machine flowchart is shown in Fig. 5(a).

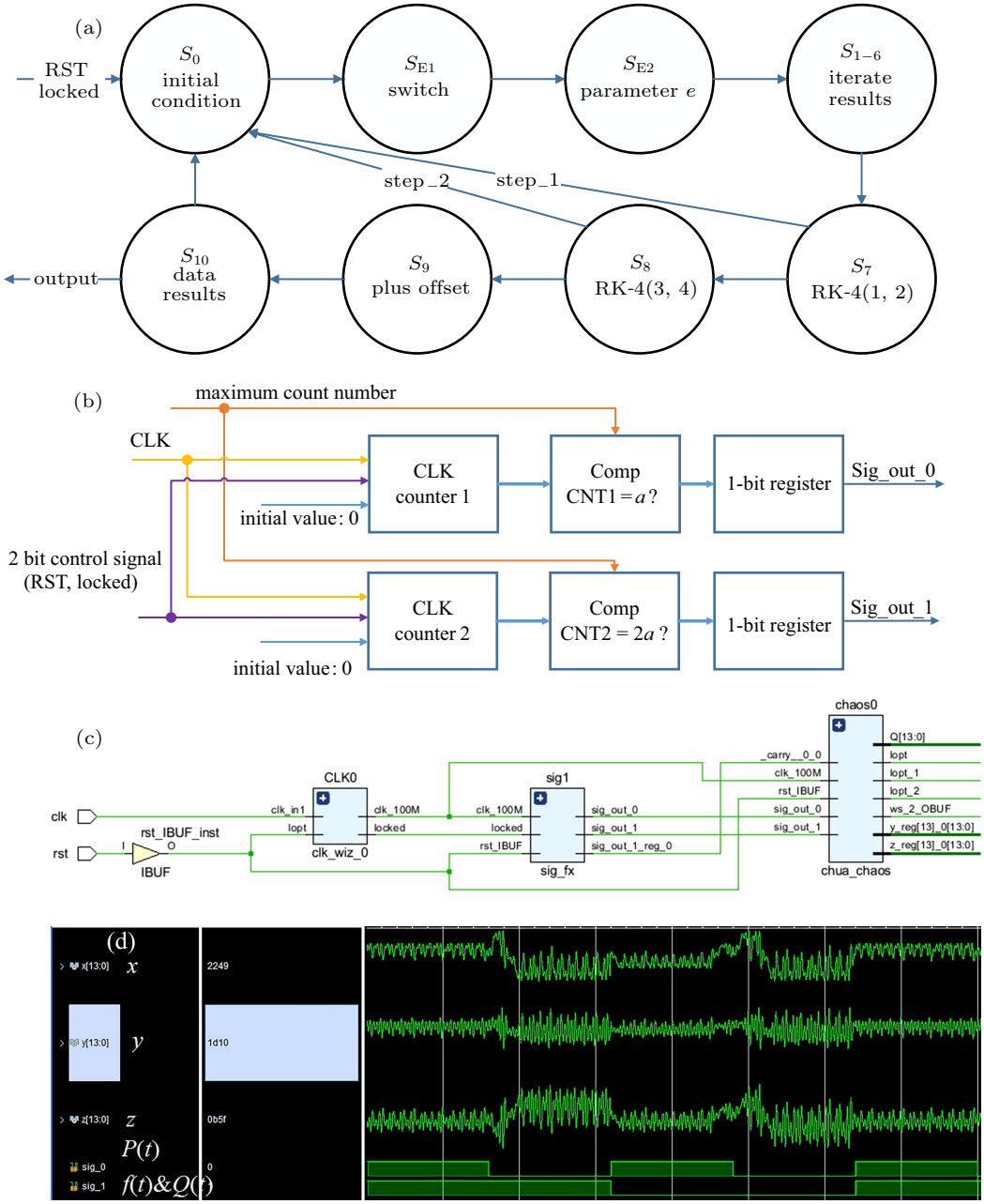


Fig. 5. (a) State machine flowchart. (b) Diagram of the PW function generator, (c) RTL diagram of the top-level module. (d) Vivado timing simulation.

The digital realization of the PW functions is presented in Fig. 5(b). Where, the generator is controlled by 2-bit signal consisting of 'RST' signal and 'Locked' signal. Two clock counters are used to count high level logic of the 'CLK' signal. When the value of a counter is equal to maximum count value, the logic level of 1-bit register, which corresponds to this clock counter, will be inverted.

The RTL diagram of top-level module is displayed in Fig. 5(c). Chaotic oscillator contains three submodules: Phase Locking Loop (PLL) module, PW function generator, and modified Chua's oscillator. In staircase function generator, the output 'sig_out_0' is used to transmission of the $P(t)$ function, and another output namely 'sig_out_1' is used to transmission of $f(t)$ and $Q(t)$ functions. Modified Chua's system contains seven output ports: three 14-bit chaotic sequences namely 'x', 'y', and 'z' and four 1-bit DAC driver signals namely 'daclk_1', 'daclk_2', 'ws_1', and 'ws_2'. Timing analysis is shown in Fig. 5(d).

4.2. Experimental results

Then, the Verilog HDL codes are synthesized and implemented by employing Xc7z020clg200 FPGA chip and AN9767 DAC chip. The resources utilization of FPGA chip is listed in Table 2 (The original system in Ref. [4] is not used FPGA to realize. In order to facilitate comparison, the original system uses the same method to realize in this work). As compared to original system, realization multi-layer nested system merely increases litter resource utilization and power consum-

ing. Digital outputs of FPGA chip are converted to analog signals by 14-bit DAC. And the experimental results are visualized by oscilloscope which are shown in Figs. 6(a) and 6(b).

Table 2. Recourse realization.

Resource	Slice LUTs	Slice registers	Slice	Bonded IOBs	Power (W)
This work	512	819	238	12	0.237
System (3)	381	690	183	12	0.235
Ref. [25]	9714	2667	5347	25	\

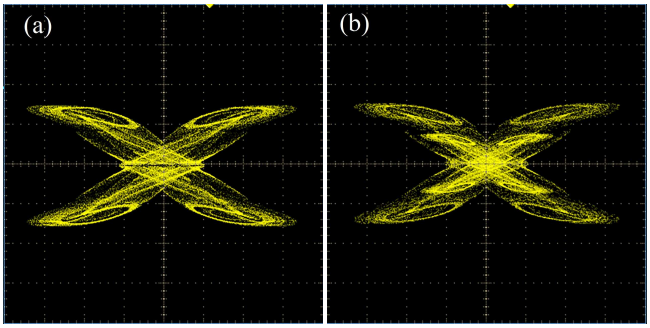


Fig. 6. (a) Mirror symmetry Chua attractor. (b) Multi-layer nested Chua's attractor.

5. Conclusion

A method to create multi-layer nested attractor is presented. Take modified Chua's system as an example, the method can be summarized in three steps. First, transforming state variables z to $-z$ for generating mirror symmetric attractors. Second, compressing state variables e times for obtaining small-amplitude attractors. Finally, introducing PW functions into system for combining above phenomena. Through employing this non-autonomous method, the modified Chua's system can create three-layer nested attractors, which have not been proposed in former works. And this method does not greatly affect the chaotic state of the system. Moreover, the approach can be applied in other chaotic systems with nested attractors. Then, the oscillator is implemented by using Xilinx Xc7z020clg200 FPGA chip. Resource consuming of novel oscillator is a little higher than the original modified Chua's system. The experimental results got by oscilloscope are the same as MATLAB simulation results, which is helpful for further real-world applications.

References

[1] Ren H P, Bai C, Tian K and Gerbogi C 2017 *Int. J. Nonlinear Mech.* **94** 334
[2] Yu F, Li L X, He B Y, Liu L, *et al*. 2019 *IEEE Access* **7** 181884
[3] Wang Z, Volos C K, Kingni S T, Azar A T *et al*. 2017 *Optik* **131** 1071
[4] Xiong L, Zhang S, Zeng Y C and Liu B C 2018 *Chin. J. Phys.* **56** 2381
[5] Deng Q L, Wang C H and Yang L M 2020 *Int. J. Bifur. Chaos* **30** 2050086
[6] Yu F, Gao L, Gu K, *et al*. 2017 *Optik* **131** 79
[7] Rajagopal K, Akgul A, Pham V T, *et al*. 2019 *Int. J. Bifur. Chaos* **29** 1950174
[8] Messias M and Reinol A C 2017 *Nonlinear Dyn.* **88** 807
[9] Zhang S, Wang X P Zeng Z G 2020 *Chaos* **30** 053129
[10] Natiq H, Said M R M, Ariffin M R K, *et al*. 2018 *Eur. Phys. J. Plus* **133** 557
[11] Pham V T, Kingni S T, Volos C K, *et al*. 2017 *AEU-Int. J. Electron. Commun.* **78** 220
[12] Zhang S, Zeng Y C and Li Z J 2018 *Chin. J. Phys.* **56** 793
[13] Munozpacheco J M, Zambranoserrano E, Volos C K, *et al*. 2018 *Chaos Solitons Fract.* **113** 69
[14] Lü J H and Chen G R 2006 *Int. J. Bifur. Chaos* **16** 775
[15] Wang C H, Hu X and Ling Z 2017 *Pramana* **88** 34
[16] Wang C H, Hu X and Ling Z 2017 *Int. J. Bifur. Chaos* **27** 1750091
[17] Zhang S, Zheng J H, Wang X P, *et al*. 2020 *Nonlinear Dyn.* **102** 2821
[18] Chen Z, Wen G L, Zhou H A and Chen J Y 2017 *Optik* **130** 594
[19] Li C B, Lu T A, Chen G R and Xing H Y 2019 *Chaos* **29** 051102
[20] Wang N, Li C Q, Bao H, *et al*. 2019 *IEEE Trans. Circuits Sys. I* **66** 4767
[21] Elwakil A S and Ozoguz S 2006 *IEEE Trans. Circuits Sys. II* **53** 862
[22] Hong Q H, Xie Q G, Shen Y and Wang X P 2016 *Chaos* **26** 083110
[23] Wu Q J, Hong Q H, Liu X Y, *et al*. 2019 *Chaos* **29** 043112
[24] Xie Q and Zeng Y C 2020 *Eur. Phys. J. Spec. Top.* **229** 1361
[25] Bao H, Hua Z Y, Wang N *et al*. 2021 *IEEE Trans. Ind. Informat.* **17** 1132
[26] Hua Z Y, Zhou Y C and Bao B C 2020 *IEEE Trans. Ind. Informat.* **16** 887
[27] Li H Z, Hua Z Y, Bao H *et al*. 2020 *IEEE Trans. Ind. Electron.*
[28] Tlelocuautle E, Rangelmagdaleno J D J, Panoazucena A D, *et al*. 2015 *Commun. Nonlinear Sci. Numer. Simulat.* **27** 66
[29] Rajagopal K, Munozpacheco J M, Pham V T, *et al*. 2018 *Eur. Phys. J. Spec. Top.* **227** 811
[30] Soloman N S, Tilba M F, Said L A, *et al*. 2018 *Proceedings of the IEEE International Symposium on Circuits and Systems (ISCAS)*, May 27–30, 2018, Florence, Italy, p. 5
[31] Dong E Z, Li R H and Du S Z 2020 *Chin. Phys. B*
[32] Wang F Q, Wang R M, Iu H H C, *et al*. 2019 *IEEE Trans. Circuits Sys. II* **66** 2062